

# Supplementary Materials

## Influence of Contacts and Applied Voltage on a Structure of a Single GaN Nanowire

Sergey Lazarev,<sup>\*,†,‡</sup> Young Yong Kim,<sup>†</sup> Luca Gelisio,<sup>†</sup> Bi Zhaoxia,<sup>¶</sup> Ali Nowzari,<sup>¶</sup>  
Ivan A. Zaluzhnyy,<sup>†</sup> Ruslan Khubbutdinov,<sup>†</sup> Dmitry Dzhigaev,<sup>†,¶</sup> Arno Jeromin,<sup>†</sup>  
Thomas F. Keller,<sup>†</sup> Michael Sprung,<sup>†</sup> Anders Mikkelsen,<sup>¶</sup> Lars Samuelson,<sup>¶</sup> and  
Ivan A. Vartanyants<sup>\*,†,§</sup>

<sup>†</sup>*Deutsches Elektronen-Synchrotron DESY, Notkestraße 85, 22607 Hamburg, Germany*

<sup>‡</sup>*National Research Tomsk Polytechnic University (TPU), Lenin Avenue 30, 634050  
Tomsk, Russia*

<sup>¶</sup>*NanoLund, Department of Physics, Lund University, P.O. Box 118, SE-221 00 Lund,  
Sweden*

<sup>§</sup>*National Research Nuclear University MEPhI (Moscow Engineering Physics Institute),  
Kashirskoe shosse 31, 115409 Moscow, Russia*

E-mail: dr.s.lazarev@gmail.com; ivan.vartanyants@desy.de

September 23, 2021

## Free-lying NWs

We have already introduced the intensity distribution around  $10\bar{1}0$  GaN Bragg peak of several free-lying NWs in the main text of the manuscript. In this section, we will present Bragg peak intensity distributions and their views from different directions of all measured free-lying NWs under investigation.

First, Bragg peaks of three NWs with diameters of 350 nm were investigated, and their diffraction patterns are shown in Figs. S1(a-c). In order to demonstrate the absence of the "double-star" structure of the Bragg reflections, which was observed in the case of bent GaN NWs, we demonstrate their view in Figs. S1(d-f) from a different angle, perpendicular to the  $[0001]$  crystallographic direction. As one can see, there is no elongation of intensity along  $[0001]$  crystallographic direction even in the case of two free-lying NWs lying close to each other in Fig. S1(f).

We also measured diffraction patterns of two GaN NWs with the diameters of 200 nm. Their intensity distributions are shown in Figs. S2(a,b). Figs. S2(c,d) show these intensity distributions from the views perpendicular to  $[0001]$  crystallographic direction. Contrary to thicker GaN NWs with diameters of 350 nm, the "double-star" structure is present in the both cases in Figs. S2(c,d).

## SEM images of the contacted NWs before and after the experiment

For each contacted GaN NW under investigation, we performed the SEM measurements before and after experiments with the applied voltage. Figs. S3(a,b) show the first 350 nm GaN NW before and after applied voltage. Figs. S3(c,d) present similar images before and after applied voltage of the second 350 nm GaN NW. Figs. S3(e,f) show the first 200 nm GaN NW before and after applied voltage.

In Fig. S4(a,b) different type of contacts with a 200 nm GaN NW on top of Au contacts before and after applied 0.1 V applied to the system "GaN NW - Au contacts" is presented. In this case, the 200 nm GaN NW was found using diffraction mapping, when the integrated scattered intensity from Au and GaN were spatially mapped on the surface of the sample. Fig. S4(c) shows a 350 nm GaN NW positioned on top of the Au contacts. This, 350 nm GaN NW was not found in diffraction mapping.

## Evolution of the scattered intensity of the NWs as a function of applied voltage

In our study, two GaN NWs with diameter of 350 nm were investigated under the applied voltage bias. The first GaN NW was already presented in the main text of the manuscript.

The second 350 nm GaN NW was measured with larger step in voltage bias and there were only two diffraction patterns recorded between 0 V and 5 V at which the NW was damaged. The intensity distribution of the second 350 nm GaN NW is shown in Fig. S5.

For both 350 nm GaN NWs, dependence of the scattering vector modulus ( $H_{10\bar{1}0}$ ) was obtained as a function of the applied voltage and is presented in Figs. S6(a,b). From this behavior, it is clearly visible that the applied voltage doesn't lead to the  $H_{10\bar{1}0}$  increase. That means that there is no increase of the unit cell lattice parameters versus current through the NWs. Therefore, we conclude that the diffraction pattern evolution is due to the piezoelectric effect and not due to increased temperature of the NWs from the current. The same behavior of the scattering vector modulus  $H_{10\bar{1}0}$  is observed for two 200 nm GaN NWs, which is shown in Figs. S6(c,d). Additionally, dependence of the bending angle of both 200 nm GaN NWs is given in Fig. S7.

## Measurements of the GaN NWs with the Pt contacts

The contacted by Au, 200 nm thick GaN nanowires were extremely sensitive to the external impact. Due to transportation of the samples from Lund to Hamburg only few out of 10 contacted NWs survived. After the measurements of these NWs with the maximum applied voltage, the NWs broke down or dis-contacted. In order to further study GaN NWs with contacts, we decided to try Pt contacts deposition on top of the 200 nm-thin GaN NWs at DESY NanoLab using Electron Beam Induced Deposition (EBID) of a Pt containing precursor material inside the SEM chamber.. The Pt contacts were deposited to the ends of the nanostructures. The SEM images of the Pt contacted 200 nm GaN NWs are shown in Fig. S8.

Due to the relatively low precision of the deposition method, the Pt material was also sputtered in the vicinity of the contacts. We expect the Pt to be deposited in a larger area around the contacts path and, thus, the whole NW was covered by a Pt layer, which should influence the conductive properties of the "GaN-contacts" system. Influence of the Pt contacts on the  $10\bar{1}0$  GaN Bragg peak is shown in Figs. S9(b,c).

As it was already discussed, the Pt material covered not only the ends of the NWs but also the whole nanostructure. Due to this reason, the NWs had an additional constraint and could not freely bend and investigation of the intensity evolution of the NWs with Pt contacts under applied voltage was not efficient enough.

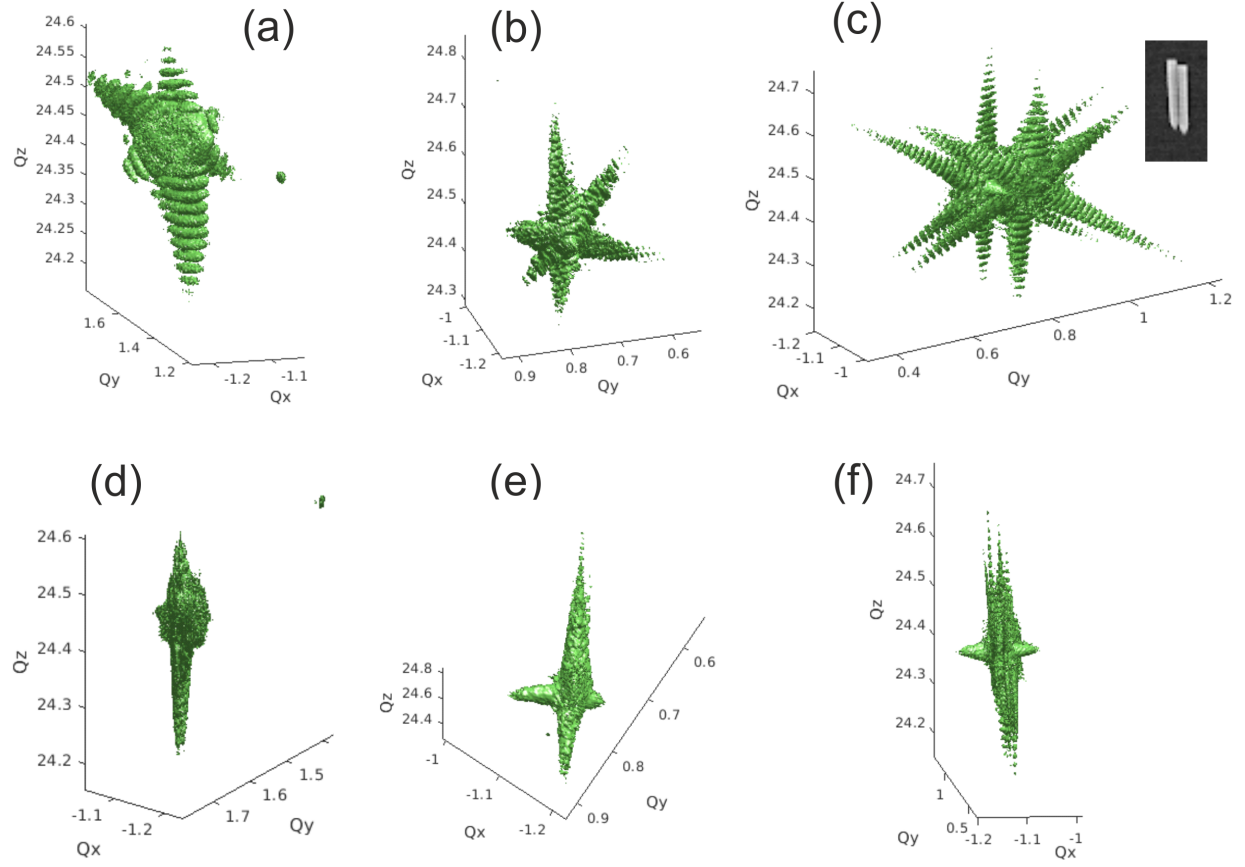


Figure S1: (a-c) The intensity distribution around  $10\bar{1}0$  GaN Bragg reflection of three different free-lying GaN NWs with diameters of 350 nm. (d-f) The same Bragg peaks from a different view perpendicular to the  $[0001]$  crystallographic direction. The figures demonstrate absence of the "double-star" structure, which was observed in the case of bent GaN NWs.

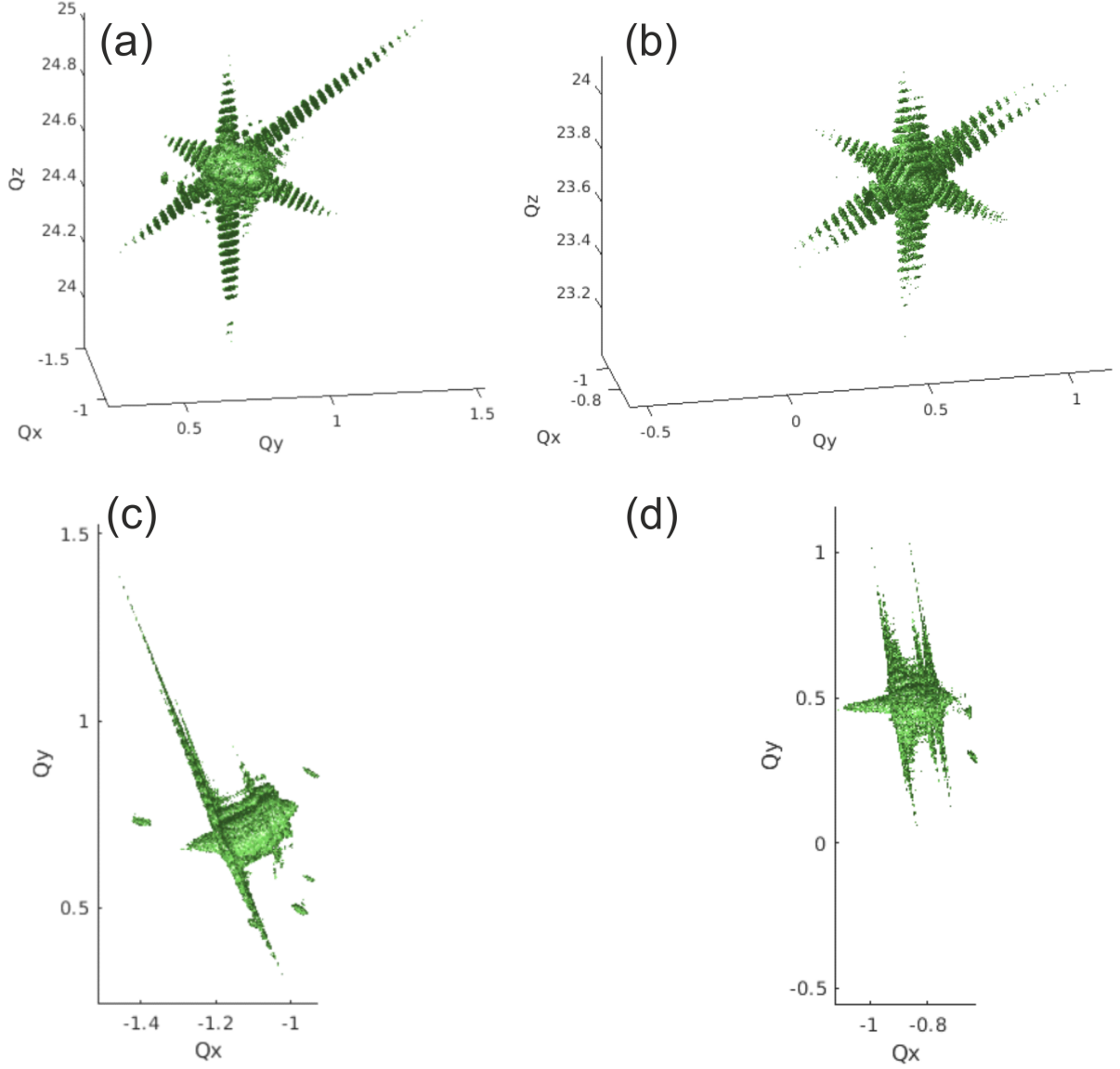


Figure S2: (a,b) The intensity distribution around  $10\bar{1}0$  GaN Bragg peak of two free-lying GaN NWs with diameters of 200 nm. (c,d) A different view of these Bragg peaks from a direction perpendicular to the  $[0001]$  crystallographic axis. The Bragg peaks demonstrate the "double-star" structure typical for the bent GaN NWs.

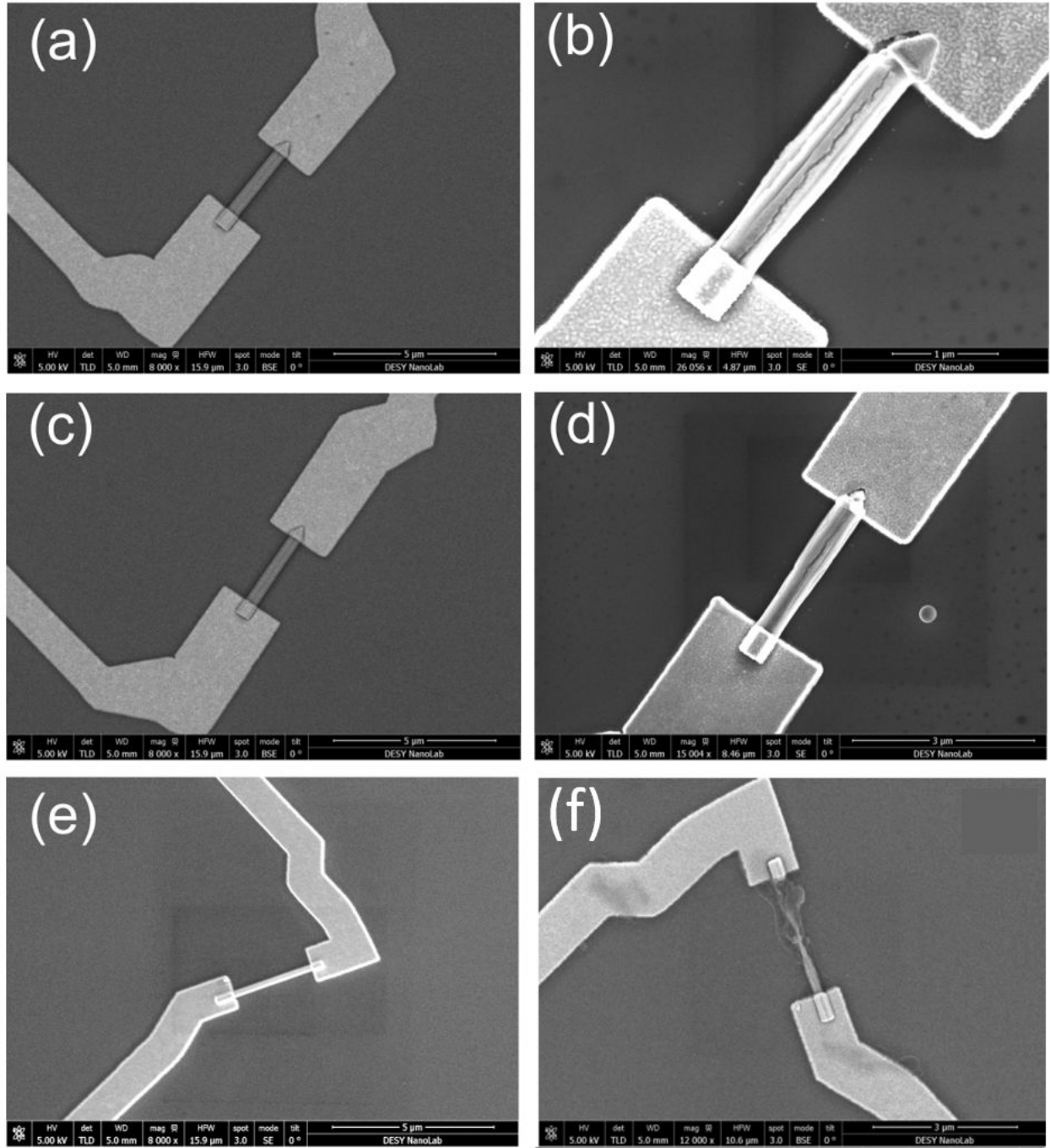


Figure S3: SEM images of the contacted GaN NWs. The first 350 nm GaN NW before (a) and after (b) applied voltage bias. The second 350 nm GaN NW before (c) and after (b) the maximum applied voltage. The 200 nm GaN NW before (e) and after (f) the applied voltage bias.

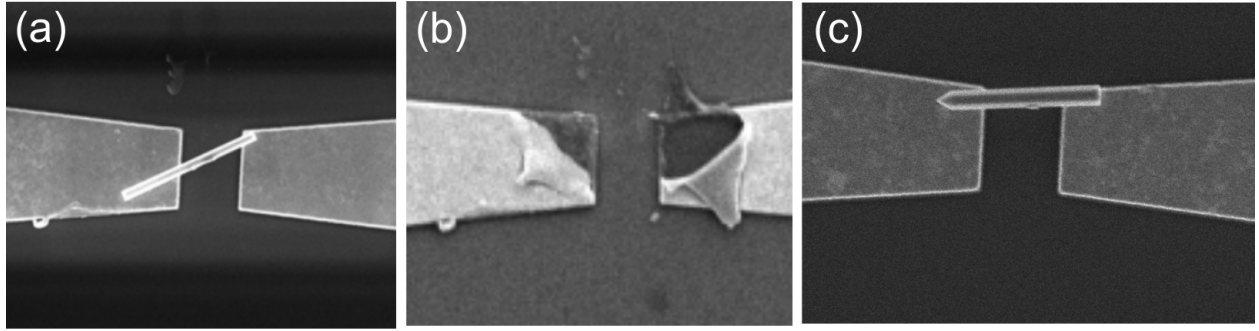


Figure S4: SEM images of the second type of Au contacts. The NW with the diameter of 200 nm contacted on the top of the Au electrodes by melting procedure before (a) and after (b) applied 0.1 V of bias. (c) The 350 nm GaN NW on the top of Au contacts.

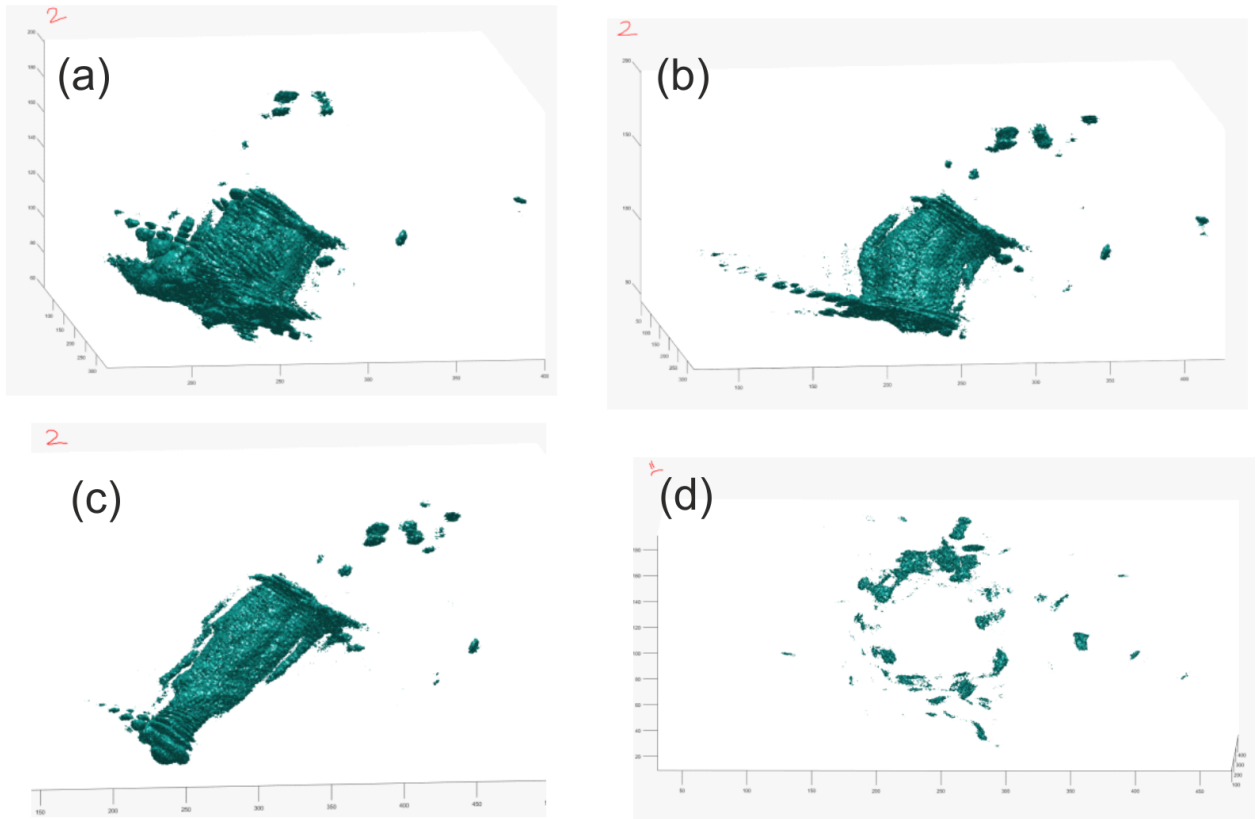


Figure S5: Evolution of the intensity distribution around  $10\bar{1}0$  GaN Bragg reflection of the second contacted GaN NW with the diameter of 350 nm. The values of the applied voltage bias: 0 V (a), 1 V (b), 2 V (c), 5 V (d).

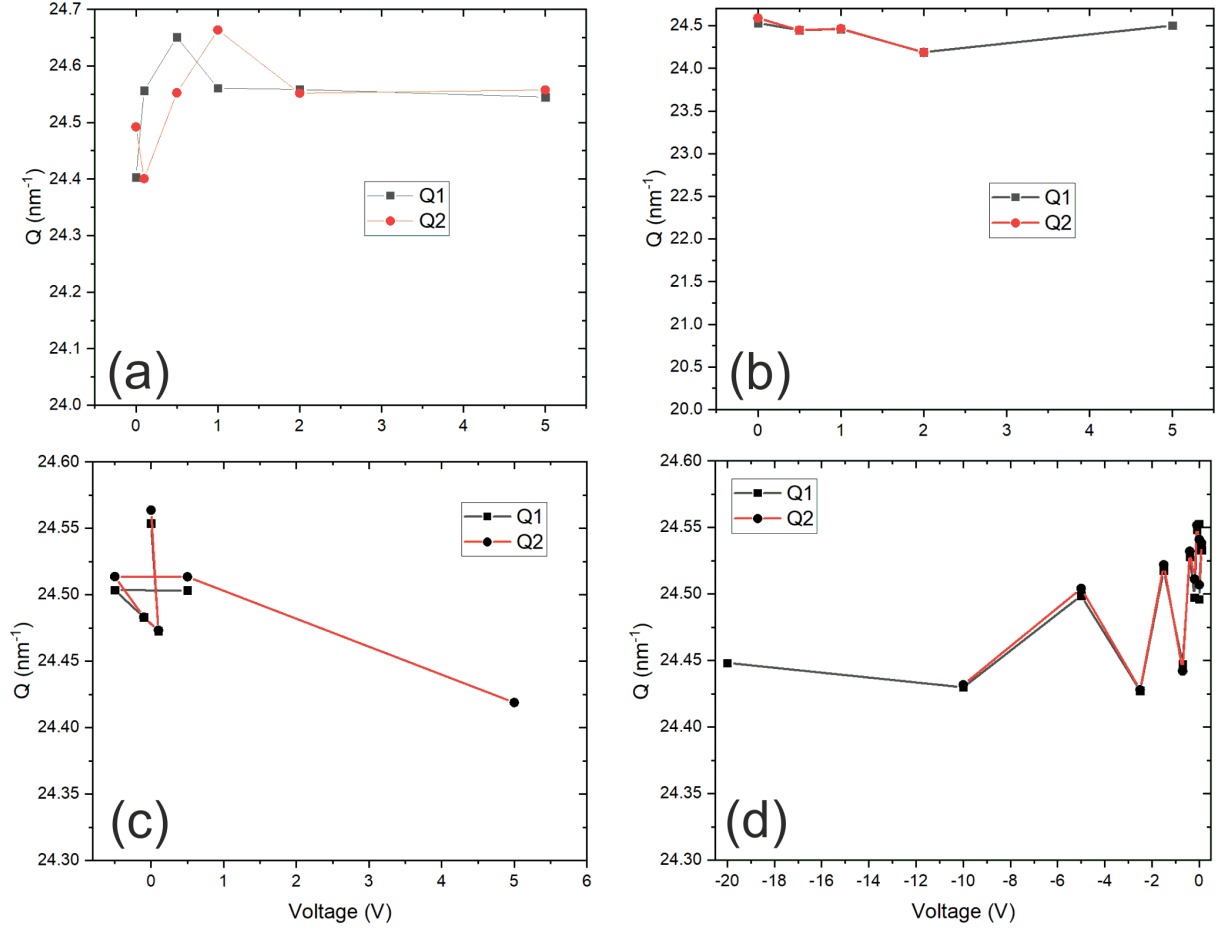


Figure S6: Dependence of the scattering vector modulus ( $H_{10\bar{1}0}$ ) on the applied voltage bias for the first (a) and second (b) 350 nm GaN NW. Similar dependence of the scattering vector modulus ( $H_{10\bar{1}0}$ ) on the applied voltage bias for the first (c) and second (d) 200 nm GaN NW.

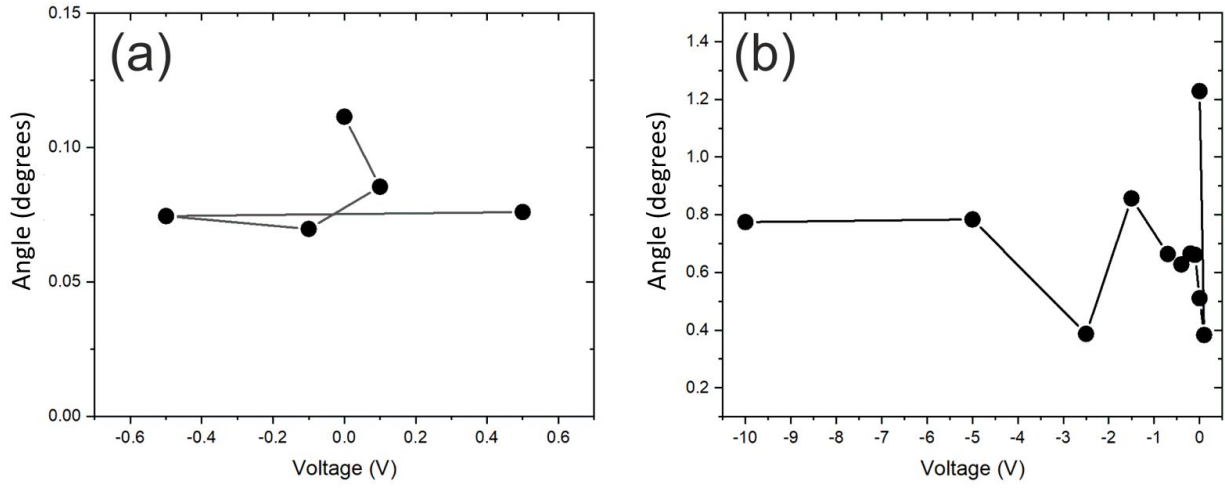


Figure S7: Dependence of the bending angle for the first (a) and second (b) GaN NW with the diameter of 200 nm on the applied voltage bias.

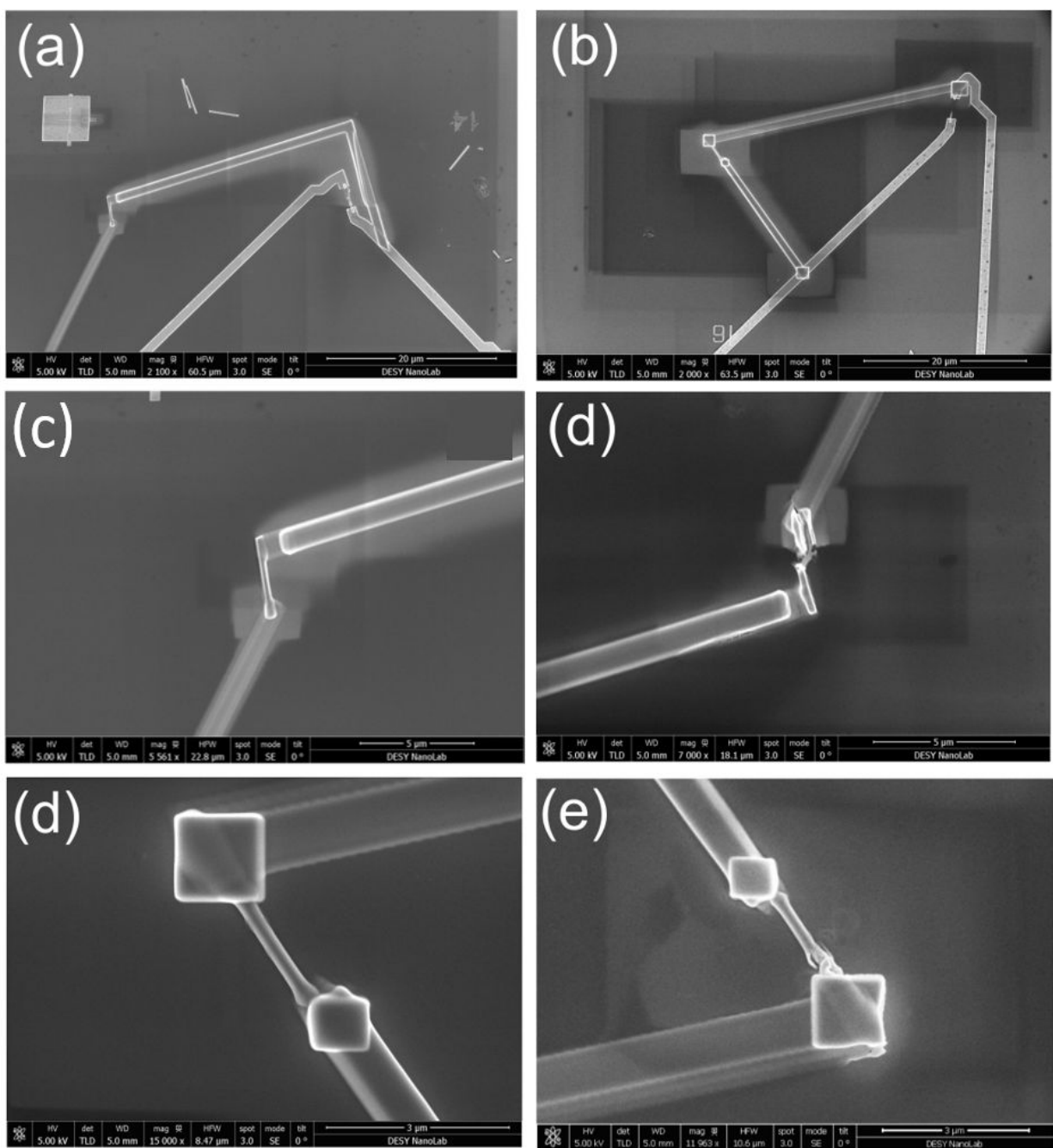


Figure S8: SEM images of the Pt contacted 200 nm GaN NWs.

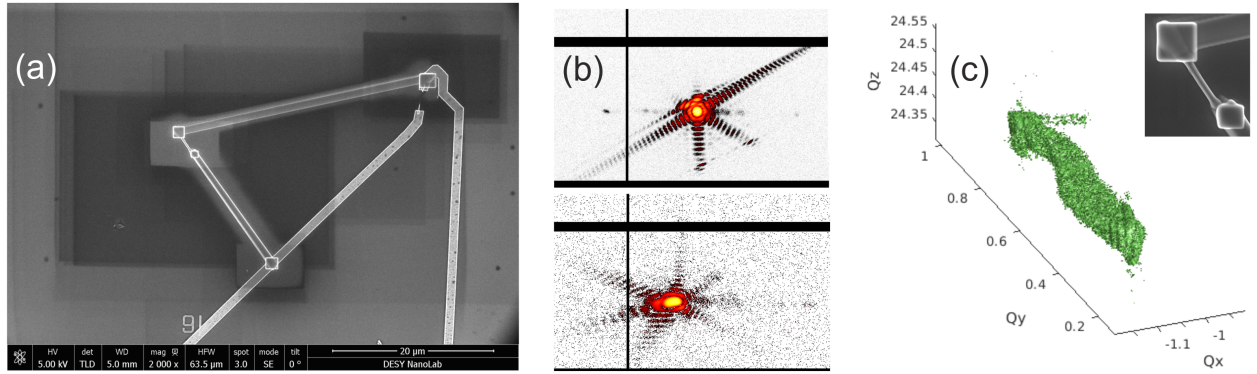


Figure S9: (a) SEM images of the Pt contacted GaN NW with diameter of 200 nm. (b) Comparison of the diffracted intensity of the  $10\bar{1}0$  GaN Bragg reflection of the NW before (up) and after (bottom) deposition of the Pt contacts. (c) 3D intensity distribution around  $10\bar{1}0$  GaN Bragg reflection of the NW.